

## EXTENDED EXPERIMENTAL PROCEDURES

### Odorant Concentration within the Trap Assay

The valence of an odorant can change depending on its concentration (Sammelhack and Wang, 2009). A changing odorant concentration over the 24h time course of the experiment could therefore change the valence. We thus tested the concentration change of 2,3-butanedione (i.e., the most volatile compound of the twelve focus odorants of this manuscript) within the trap assay during more than 24 hr. The treatment trap contained 2  $\mu$ l of the test odorant diluted in 200  $\mu$ l of water (plus 0.2  $\mu$ l Triton X-100 (<http://www.sigmaaldrich.com>)). We sampled odorant concentration every 1-to-2 hr in the pipette tip forming the entrance to the trap and outside in the box containing the flies initially using a Solid Phase Micro Extraction (SPME) fiber (100 $\mu$ m PDMS; Supelco 57341U). We proceeded to quantify the accumulated odorant molecules on the fiber using gas chromatography (GC; Agilent 6890N) in combination with mass spectrometry (MS; Agilent MS 5975B) running the following protocol:

Desorption within GC inlet, 1 min; GC program: 2 min at 40°C followed by increasing temperature (20°/min up to 280°C) and a final step of 5 min at 280°.

The concentration was constantly higher within the tip than outside in the box, and decreased less than 1 order of magnitude during 24 hr (Figure S1). Especially during the first 4 hr, during which most of the flies typically respond in the trap assay (Ruebenbauer et al., 2008), the decrease of odorant concentration was negligible. Consequently, irrespective whether the flies responded at the beginning of the experiment or later, they always experienced comparable concentrations.

### Identification of Glomeruli

Wide field microscopy provides a highly convenient and reliable overview of neuronal activity evoked by a specific odorant among a large number of olfactory glomeruli. As an alternative, the two-photon system offers more information due to the capability of deep optical sectioning through different layers of glomeruli. Since we have both techniques available, a wide field and a two-photon imaging system, we have performed calcium imaging experiments and monitored the odorant-evoked calcium responses of a fly antennal lobe expressing the calcium sensor G-CaMP in OSNs using both systems (Strutz et al., 2012).

We found that the glomeruli strongly activated by a specific odorant can be individually and unambiguously identified using both systems (see Figure 1 in Strutz et al., 2012). We performed this comparison for a number of odorants including some of those used in the present study and did not find any differences for the glomeruli under investigation.

A potential drawback of wide-field imaging is, that only superficial glomeruli are accessible with this technique. However, the superficial glomeruli that are accessible in wide field imaging cover about 60% of glomeruli labeled by the Orco-GAL4 as well as the GH146-GAL4 driver lines, which we find is sufficient to allow conclusions regarding coding strategies in the antennal lobe. The more ventrally located glomeruli (that are not visible in wide field imaging) are mainly innervated by IR-expressing OSNs and are thus not labeled by Orco-GAL4 (Silbering et al., 2011; Couto et al., 2005). We therefore decided to apply wide field calcium imaging for the glomerular characterization. In addition the effect of light scattering that arises when using wide field imaging occurs at both the OSN and the PN level and is thus compensated by comparing both data sets.

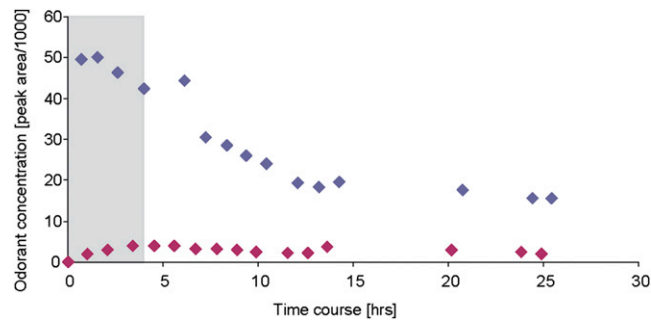


**Figure S1. Concentration Change over the 24 hr Time Course of the Trap-Assay Experiment, Related to Figure 1**

Blue diamond, concentration measured within the entering tip of the trap; red diamond, concentration measured within the box containing the flies initially; gray rectangle, time window during which most flies enter a trap in this kind of trap assay (Rübenbauer et al., 2008). Concentration is depicted as the area below the odorant peak that resulted from the GC analysis. Please note that we could not sample odorants at both positions simultaneously. Therefore, consecutive sampling in box and tip was separated by 30 min.

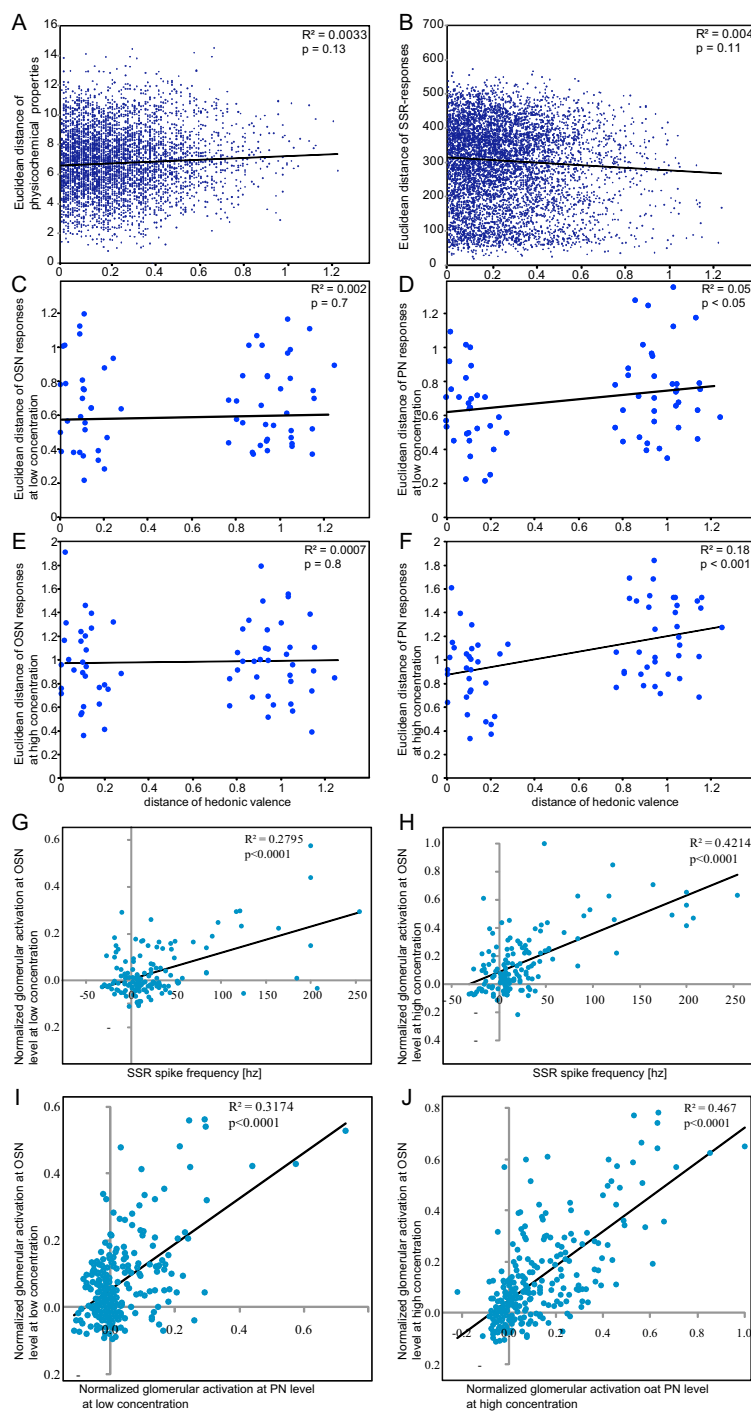


**Figure S2. Correlation Analyses, Related to Figure 4**

(A–F) Correlation of Euclidean distances calculated based on physicochemical or physiological properties and the distances based on hedonic valences of odorant pairs. (A) Physicochemical properties. For the set of 110 odorants Euclidean distance for each possible odorant pair was calculated based on 32 physicochemical descriptors (Haddad et al., 2008). (B–F) Physiological properties. (B) For the same set of odorant pairs Euclidean distance was calculated based on published single sensillum recordings (Hallem and Carlson, 2006). (C–F) Euclidean distance was calculated for those twelve odorants which we used with low and high concentration for the imaging experiments based on OSN responses (C and E) and PN responses (D and F). The only significant correlation was found on the level of PNs.

(G and H) Correlation between activation patterns measured at the input level (OSN) of the antennal lobe and published single sensillum recordings (Hallem and Carlson, 2006).

(I and J) Correlation between activation patterns of OSNs and PNs.

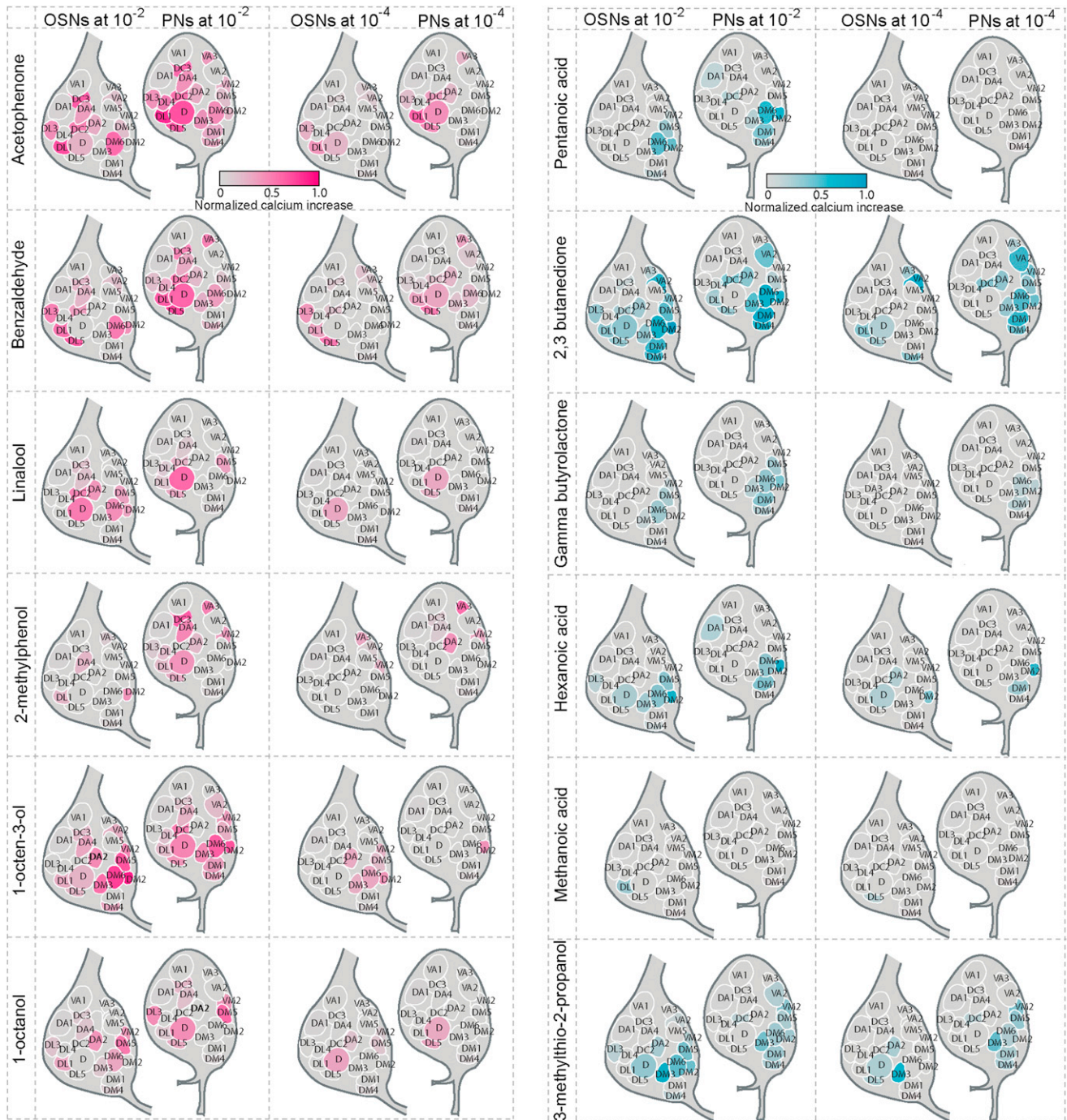


**Figure S3. Activation Patterns after Stimulation with Aversive and Attractive Odorants at the Level of OSNs and PNs, Related to Figure 3**  
Columns 1 and 2, aversive; columns 3 and 4, attractive. Columns 1 and 3, high stimulus concentration ( $10^{-2}$ ); columns 2 and 4, low stimulus concentration ( $10^{-4}$ ). Stimulus duration, 2 s.